Program Digest, 2019 IEEE International Ultrasonics Symposium (IUS)
Glasgow, Scotland, October 6-9, 2019

SAW 4.3 GHz Delay Line and Reflector Design Results

Michael J. Morales Otero
Electrical & Computer Engineering Department
University of Central Florida
Orlando, FL. USA
mj.morales@knights.ucf.edu

Luis M. Rodriguez Cordoves
Electrical & Computer Engineering Department
University of Central Florida
Orlando, FL. USA
luismrodriguez@gmail.com

Arthur R. Weeks
Electrical & Computer Engineering Department
University of Central Florida
Orlando, FL. USA
arthur.weeks@ucf.edu

Donald C. Malocha
Pegasense LLC.
Orlando, FL. USA
dcmalocha@cfl.rr.com

***Abstract*—Surface acoustic wave (SAW) sensors provide wireless and passive operation within small embodiments. With the recent adoption of the 4.2 to 4.4 GHz band for Wireless Avionics Intra-Communication (WAIC), SAW sensors are a promising solution for current and future demands of this application. Although some experiments on SAW sensors have been done at GHz frequencies, very little is known about SAW propagation, important parameters, and properties at these frequencies. No SAW sensors have been demonstrated at WAIC frequencies up to date.**

This paper presents the design and analysis of SAW delay lines, and reflector devices at 4.3 GHz. Unmatched SAW delay line response having 33 dB loss has been achieved; even though this may seem high – it is acceptable for SAW sensors within near-field ranges expected in air- and space- craft frames. SAW device simulation using the coupling of modes (COM) model [1], device fabrication feasibility, preliminary measurements, and a demonstration of wireless sensor operation at 4.3 GHz will be given. Transducer design topologies explored are shown with validation of transduction coupling at harmonics. Device embodiment and antenna design will also be presented.

Keywords*— *SAW, WAIC, 4.3 GHz, sensors, UCF

I. Introduction

Surface acoustic wave (SAW) sensors are one solution for sensor technology demands, given that SAW sensors allow for passive operation, small embodiments, and versatility [2]. With the recent adoption of the 4.2 to 4.4 GHz band for Wireless Avionics Intra-Communication (WAIC), SAW sensors are one possible solution for advancing this technology. Wireless sensor operation, in avionics, is extremely desirable and advantageous as it improves safety and reliability while reducing weight, cost, and maintenance of wired sensors. Moreover, wireless sensor operation also provides a greater redundancy in monitoring systems.

This paper presents design, simulation, fabrication, and testing of 4.3 GHz SAW delay lines and reflector devices. Different transducer designs are analyzed for different harmonic operation and metallization ratios (a/p ratio). Devices are fabricated and preliminary measured to validate theory of transduction at harmonic frequencies. The coupling of modes (COM) predictions are provided and compared with device measurements. An antenna design at operating frequency of 4.3 GHz is developed and fabricated for enabling sensor wireless operation. Demonstration and operation of an initial 4.3GHz temperature sensor is also shown.

II. Design and Fabrication

Device fabrication begins with a mask that is produced using an Electromask pattern generator and image repeater. First, a reticle is fabricated with the pattern generator that produces rectangular flashes of UV light over a chromium-coated glass plate with photoresist. The reticle has device features 10x larger than the desired size. The reticle is chrome-etched and then used in an image repeater to flash the pattern over the mask plate. The pattern is optically reduced 10x producing the desired size. The mask is developed, and chrome etched to resolve the devices. Photolithography process and E-beam is used to transfer the mask pattern to a lithium niobate wafer.

Initial 4.3 GHz devices were designed and fabricated to characterize their behavior. Given fabrication limitations at fundamental device wavelengths [3], the devices were designed to operate at harmonic frequencies (fabricated at lower frequencies). The critical dimension (CD) of an interdigital transducer (IDT) is given by [1]:

$$CD_n = n\frac{\lambda}{2S_e} \tag{1}$$

$$\lambda = \frac{v_{IDT}}{f_0} \tag{2}$$

where n is the harmonic number, λ the wavelength, S_e the number of electrodes per λ (2 or 4), v_{IDT} the acoustic wave velocity under the IDT, and f_0 the center frequency of the SAW structure.

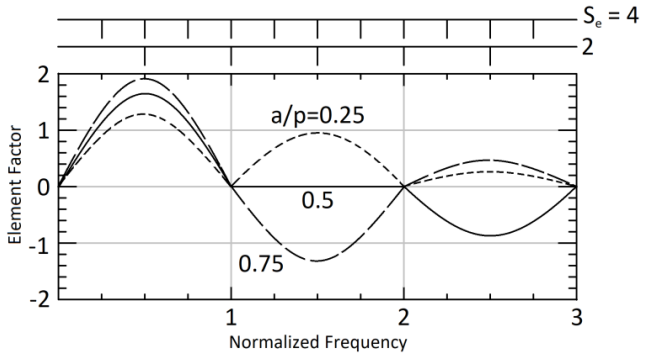

Figure 1: Element factor for an interdigital SAW transducer [1].

This work was supported under a NASA SBIR contract, 80NSSC18P2177, "4.3 GHz Passive Wireless Sensor System".

For $\lambda/8$ IDTs ($S_e = 4$), 7th harmonics and higher meet the required fabrication constrains (0.7um feature size for the image repeater). For $\lambda/4$ IDTs ($S_e = 2$), 3rd harmonics and higher also meet these fabrication constrains. The harmonics present in an IDT response depend on the element and array factors of an IDT. Figure 1 shows the element factor of an IDT for $2f_0$ and $4f_0$ transducers for different a/p ratios [4]. The array factor for $\lambda/4$ and $\lambda/8$ devices show that even harmonics are not present in an IDT response. Using the smallest feature size allowed by the required fabrication process, the element factor, and the array factor of transducers, the most feasible combination of harmonics and a/p ratios were selected as 75% for $\lambda/4$ - 3rd harmonic, as 50% for $\lambda/4$ - 5th harmonic, as 75% for $\lambda/8$ - 7rd harmonic, and as 50% for $\lambda/8$ - 9th harmonic.

III. Results and Analysis

A. Measurements

Fabricated devices were measured on wafer using an RF probe station. Measurements show that the harmonic response is very sensitive to the a/p ratio. For $4f_0$ transducers with a fundamental frequency of 477.7 MHz, 5th and 7th harmonics are present with a/p ratio closer to 75%, but eliminated or largely attenuated when a/p ratio is 50% as shown in figure 2 and figure 3.

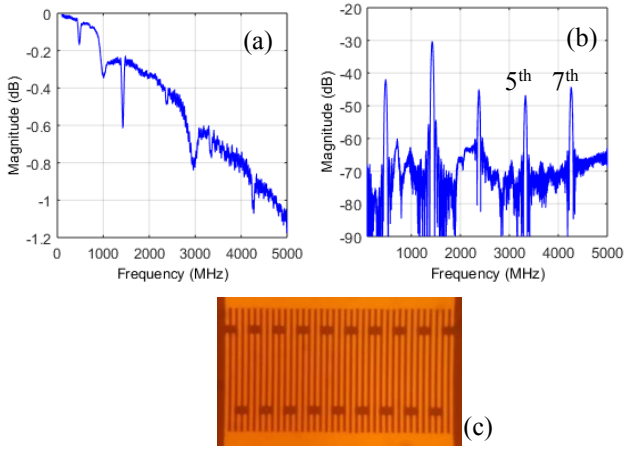

Figure 2: S11 and S21 parameters (a) and (b), respectively, of a two-port 9th harmonic device having approximately 65% a/p ratio electrodes. A micrograph of a $4f_0$ IDT is shown in (c).

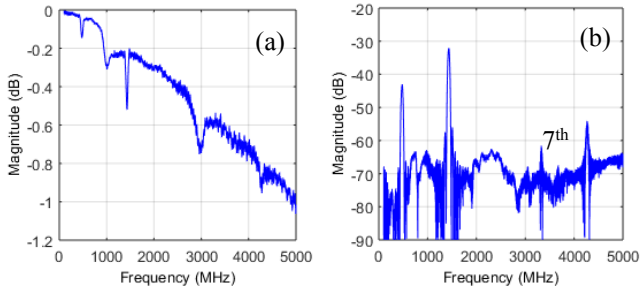

Figure 3: S11 and S21 parameters (a) and (b), respectively, of a two-port 9th harmonic device having approximately 50% a/p ratio electrodes.

Two-port delay line with $2f_0$ transducers are presented in figure 4 and 5 with approximately 75% and 50% a/p ratio, respectively. The theory of harmonic response generation for SAW transducers shows good agreement in that a $2f_0$ transducer should have a strong 3rd harmonic and a weaker 5th harmonic response when the a/p ratio is near 75%. A strong 5th harmonic response is also obtained for the $2f_0$ IDT when the a/p ratio is close to 50%, while there is little to no 3rd harmonic response.

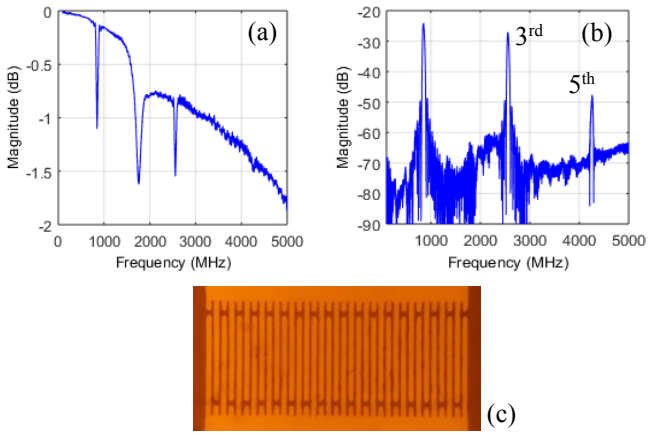

Figure 4: S11 and S21 parameters (a) and (b), respectively, of a two-port 5th harmonic device having approximately 70% a/p ratio electrodes. A micrograph of a $2f_0$ IDT is shown in (c).

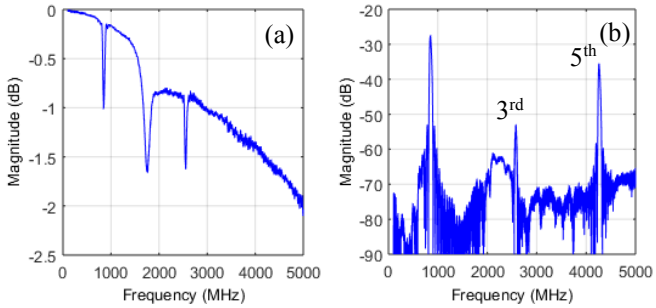

Figure 5: S11 and S21 parameters (a) and (b), respectively, of a two-port 5th harmonic operational device at 4.3 GHz having approximately 55% a/p ratio electrodes.

A one-port, $2f_0$, 5th harmonic reflective delay-line device with 50% a/p ratio was designed, fabricated, and used as a wireless SAW temperature sensor. The reflector used is a uniform Bragg reflector. $2f_0$ 5th harmonic reflectors provide good harmonic response at 4.3 GHz while meeting fabrication limits. The device layout, S11 frequency response, and time domain response are shown in figure 6. The COM model was used for sensor simulations and compared to the measured response.

B. COM Model

The COM model for the one-port, $2f_0$ *sampled IDT*, 5th harmonic operating reflective delay-line was developed for simulations. The device probe pad parasitics were extracted from open and shorted pad structures on the device wafer. Figure 7 shows the circuit model used for parasitics extraction. C_p, the pad capacitance, is obtained from the open pad S_{11} parameter. R_p and L_p, pad resistance and inductance

respectively, are obtained from the shorted S_{11} parameter. The measured and circuit model impedances are matched to derive the parasitics parameters.

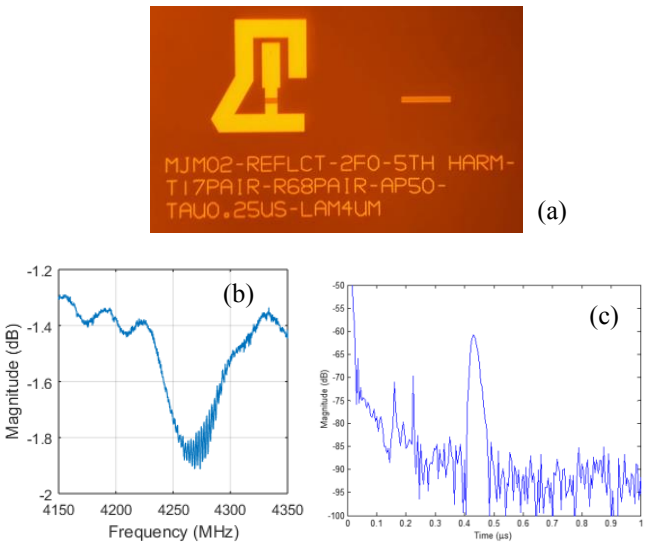

Figure 6: Device layout of reflective delay-line sensor (a). The transducer has 17 electrode pairs and the reflector has 138 strips. A measured device S11 response having this topology is shown in frequency (b) and time (c).

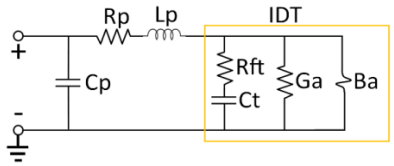

Figure 7: Circuit model used to calculate contact and probe pad parasitics. The IDT portion of the circuit is not used.

The measured SAW sensor device and the COM model simulation plots are given in figure 8 for both the time and frequency response.

IV. Sensor Embodiment and Antenna Design

The one-port 5th harmonic device is used as a 4.3 GHz temperature sensor. The fabricated SAW sensor is mounted inside a gold package and then wire bonded to external pins. This package is then sealed and connected to an external SMA connector. Figure 9 shows the 4.3 GHz sensor package with an external SMA connector.

A 4.3 GHz dipole antenna is designed and fabricated for the wireless SAW sensor and for the wireless interrogation system developed at the University of Central Florida. Figure 10 shows the antenna layout designed in ANSYS [5] and figure 11 shows the antenna simulation and measured S11 responses. The antenna was fabricated and soldered to an SMA cable, and S11 was measured using a VNA.

The antenna was designed and simulated at a lower frequency of 4.14 GHz and then tuned to achieve a center frequency of 4.3 GHz. The measured response shows -21.9 dB (-26.5 dB simulated) of reflection at this center frequency and a 400 MHz (500 MHz simulated) of 10 dB bandwidth.

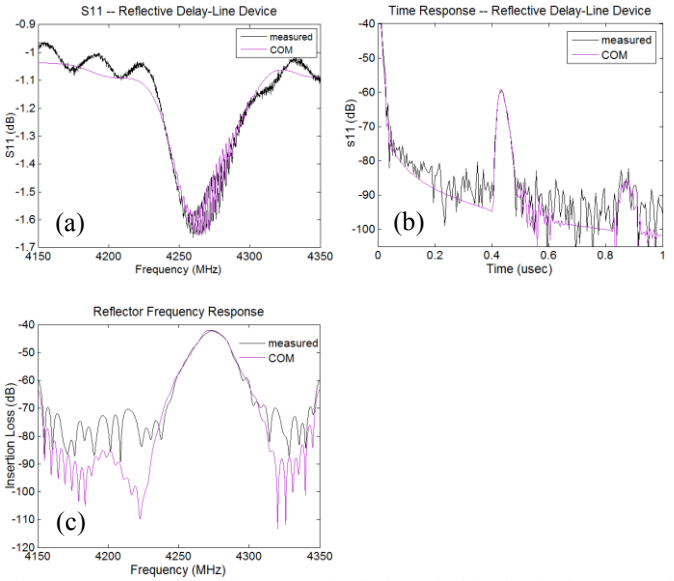

Figure 8: One-port delay-line COM simulation. The blue line is the measured response and the purple line is COM model simulation

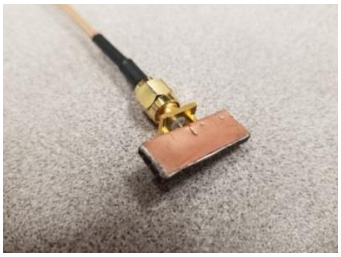

Figure 9: 4.3 GHz SAW temperature sensor packaged.

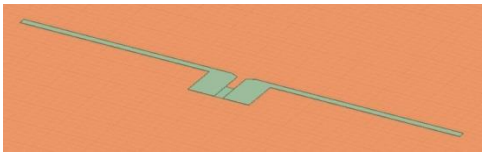

Figure 10: 4.3 GHz dipole antenna design using ANSYS.

V. Sensor Test Setup and Measurement

Figure 12 shows the wireless testing of 4.3 GHz temperature sensor. A VNA is used for reading the time response of the sensor along with two 4.3 GHz dipole antennas which are are used by the sensor and the VNA. Signal from the sensor is observed on the VNA from the sensor when both antenna dipoles are parallel to each other and goes to zero when the atenna dipoles are placed orthogonally to other.

To read the sensor temperature, a prototype 4.3 GHz interrogation system was developed by UCF CAAT [6]. Figure 13 shows the diagnostic plots of the interrogation system. The sensor is interrogated using a chirp signal with a 35 MHz bandwidth and a 0.25 µs duration (time domain raw plot – top left). Time domain (processed) plot is the deconvolved raw signal (top right). The frequency domain plot (bottom left) is the frequency response of the signal gated around the sensor frequency of operation, and the frequency

scaling factor plot shows the correlation between the matching filters (one for each unique temperature) and the sensor response (bottom right). The peak indicates the best correlation with sensor signal and the given matched filter. From the best selected match filter the sensor temperature is extracted.

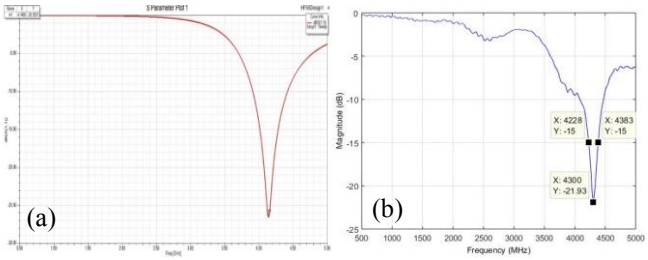

Figure 11: Simulated (a) and measured (b) S11 for a new 4.3 GHz dipole antenna.

Figure 14 shows the 4.3 GHz temperature sensor response when heated up multiple times with a heat gun and left to cool down to room temperature. The plot represents a relative temperature that can be calibrated to absolute temperature.

CONCLUSION

Different SAW device topologies were evaluated for harmonic response at 4.3 GHz, achieving 33 dB unmatched device loss. This loss, although seems high, is acceptable for near-field ranges expected in air- and space- craft frames. A COM model was developed for validation of device measurements. A dipole antenna was designed and fabricated at 4.3 GHz to enable wireless operation of the SAW reflective device. A wireless SAW temperature sensor was successfully tested using the UCF sensor interrogation system and temperature sensing with 4.3 GHz SAW device is demonstrated.

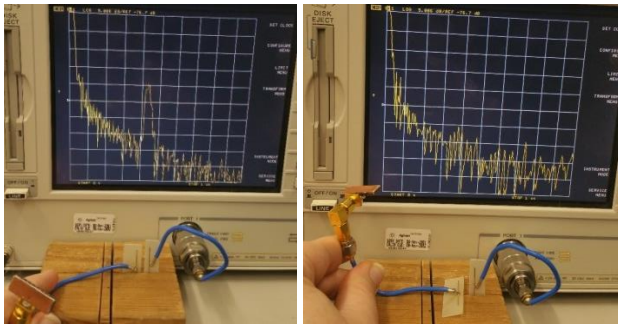

Figure 12: Testing a 4.3 GHz SAW sensor with an antenna. The VNA and the packaged device are connected to two equal 4.3 GHz dipole antennas using short blue SMA cables. Left: antennas are same oriented. Right: antennas are orthogonally oriented.

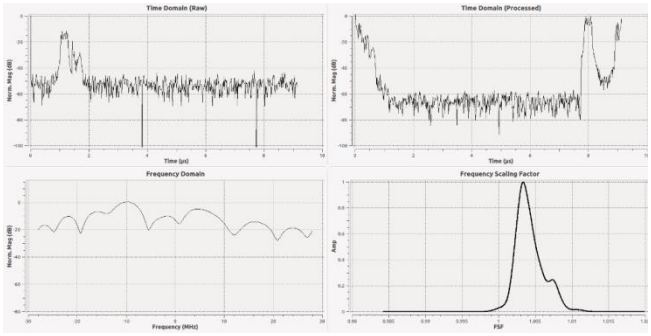

Figure 13: UCF SAW sensor interrogation system (diagnostic plots). Top left: Time domain raw data. Top right: Time domain processed data. Bottom left: Frequency domain data. Bottom right: Frequency scaling factor (FSF).

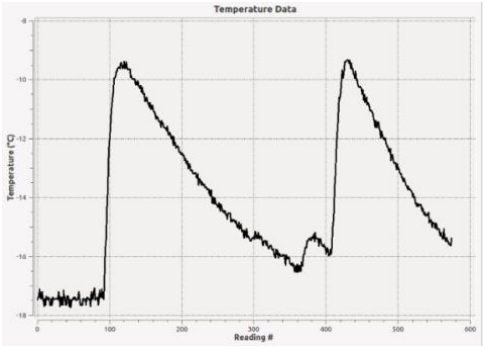

Figure 14: Temperature response of a 4.3 GHz temperature sensor.

ACKNOWLEDGMENT

The authors would like to thank Pegasense and NASA for the support and funding of this work through a NASA SBIR project.

REFERENCES

[1] C. S. Hartmann, P. V. Wright, R. J. Kansy and E. M. Garber, "An Analysis of SAW Interdigital Transducers with Internal Reflections and the Application to the Design of Single-Phase Unidirectional Transducers," 1982 Ultrasonics Symposium, San Diego, CA, USA, 1982, pp. 40-45.

[2] J. R. Humphries and D. C. Malocha, "Wireless SAW Strain Sensor Using Orthogonal Frequency Coding," in IEEE Sensors Journal, vol. 15, no. 10, pp. 5527-5534, Oct. 2015.

[3] D. R. Gallagher, M. W. Gallagher, N. Saldanha, J. M. Pavlina and D. C. Malocha, "Spread Spectrum Orthogonal Frequency Coded SAW Tags and Sensors Using Harmonic Operation," in IEEE Transactions on Microwave Theory and Techniques, vol. 58, no. 3, pp. 674-679, March 2010.

[4] D. Morgan, "Surface Acoustic Wave Filters: With Application to Electronic Communications and Signal Processing" pg. 134. Academic Press, 2007.

[5] Al-Rizzo, Hussain. (2004). "Simulations of Dipole Antennas Using HFSS". 10.13140/RG.2.1.4172.5602.

[6] D. C. Malocha, J. Humphries, J. A. Figueroa, M. Lamothe and A. Weeks, "915 MHz SAW wireless passive sensor system performance," 2016 IEEE International Ultrasonics Symposium (IUS), Tours, 2016, pp. 1-4.